

# Post-processing of structural MRI for individualized diagnostics

Pascal Martin<sup>1</sup>, Benjamin Bender<sup>2</sup>, Niels K. Focke<sup>1</sup>

<sup>1</sup>Department of Neurology and Epileptology, Hertie Institute for Clinical Brain Research, <sup>2</sup>Department of Diagnostic and Interventional Neuroradiology, University of Tübingen, 72076 Tübingen, Germany

*Correspondence to:* Pascal Martin, MD. Department of Neurology and Epileptology, Hertie Institute for Clinical Brain Research, University of Tübingen, Hoppe-Seyler Strasse 3, 72076 Tübingen, Germany. Email: pascal.martin@med.uni-tuebingen.de.

**Abstract:** Currently, a relevant proportion of all histopathologically proven focal cortical dysplasia (FCD) escape visual detection; this shows the need for additional improvements in analyzing MRI data. A positive MRI is still the strongest prognostic factor for postoperative freedom of seizures. Among several post-processing methods voxel-based morphometry (VBM) of T1- and T2-weighted sequences and T2 relaxometry are routinely applied in pre-surgical diagnostics of cryptogenic epilepsy in epilepsy centers. VBM is superior to conventional visual analysis with 9-15% more identified epileptogenic foci, while T2 relaxometry has its main application in (mesial) temporal lobe epilepsy. Further methods such as surface-based morphometry (SBM) or diffusion tensor imaging are promising but there is a lack of current studies comparing their individual diagnostic value. Post-processing methods represent an important addition to conventional visual analysis but need to be interpreted with expertise and experience so that they should be apprehended as a complementary tool within the context of the multi-modal evaluation of epilepsy patients. This review will give an overview of existing post-processing methods of structural MRI and outline their clinical relevance in detection of epileptogenic structural changes.

**Keywords:** Epilepsy; post-processing; voxel-based morphometry (VBM)

Submitted Dec 08, 2014. Accepted for publication Jan 28, 2015.

doi: 10.3978/j.issn.2223-4292.2015.01.10

View this article at: <http://dx.doi.org/10.3978/j.issn.2223-4292.2015.01.10>

## Introduction

Focal epilepsy (FE), i.e., seizures originating from a local brain region, is the most common type of epilepsy and represents about two thirds of patients. One of the main underlying causes of FE is the disruption of cortical architecture and is found under the umbrella term malformations of cortical development (MCD). This is the most important etiology for drug resistant epilepsy in childhood with more than 50% and the second to third most important cause in adults with 15-20% of all cases (1-3). MCD represent a heterogeneous group of structural changes of the cortical architecture in a wide spectrum ranging from macroscopically visible alterations to microscopic changes on cellular level with loss and misplacement of cells or disruptions to the

cortical lamination. Focal cortical dysplasia (FCD) is the largest subgroup of MCD and poses special challenges for neuroimaging and therapy in epilepsy. The etiology of these FCDs is still not sufficiently clear. Beside environmental causes, e.g., due to intrauterine infection or cerebral ischemia, there are possible signs of genetic involvement as there are descriptions of dysfunction in signaling pathways such as Wnt, NOTCH or mTOR, that influence migration of neurons (4). FCDs can be further classified histopathologically (5). The recently revised 2011 ILAE classification comprises of three main types of FCD (1= FCD with abnormal radial and or tangential cortical lamination, 2= FCD with dysmorphic neurons with or without balloon cells, 3= FCD in association with a principal lesion as hippocampus sclerosis, glial or glioneuronal tumor, vascular malformation or any other

lesion acquired during early life). FCDs are intrinsically epileptogenic (6,7) and lead to epilepsy in at least 75% of cases (8) that can manifest at any age. Furthermore, epilepsies due to FCD are often difficult to treat sufficiently with antiepileptic drugs. If an FCD can be identified as a trigger for seizures in accordance to EEG and clinical criteria and is located in a non-essential region, the therapy of choice for drug resistant epilepsy would be the surgical resection, usually including surrounding brain tissue (topectomy, lobectomy). Postoperative freedom from seizures depends, among others, on the type of the FCD, as FCD type IIb is shown to be associated with a higher probability of seizure-free outcome (9). Presently 25-80% of operated patients achieve seizure freedom (10,11). Among patients with relapsing seizures a subtotal resection can be histopathologically proven in at least 30% of patients (12,13), even if the preoperatively identified lesion could be resected in total (14). This shows that using state-of-the-art preoperative imaging, the true extent of FCD cannot be adequately detected in many cases and, thus, resections of the epileptogenic region may be incomplete. The fact that routine clinical diagnostic tools fail to detect many FCDs so that patients cannot be offered a potentially curative surgical therapy (15) is equally relevant.

MRI is the diagnostic tool in detecting structural lesions like FCD. A positive lesion identification in MRI is the best prognostic factor for post-operative seizure freedom (16). To some extent FCDs show characteristic changes such as thickening/atrophy of the cortical band, hyperintensity in T2-weighted sequences or blurring of the grey/white matter junction zone (11,17,18). However, MRI features do not always coincide to the histopathological classification (19). Further neuroimaging methods potentially increasing sensitivity for detection of epileptogenic lesions are FDG-PET (20) and MEG (7), however, due to low availability, their role in clinical routine diagnostics is currently limited. MR-technical advances, such as higher magnetic field strengths, enabled a substantial improvement in detection rates (21). Knake *et al.* (22) could show that 3 tesla MRI was able to detect FCDs in 65% of cases which were evaluated as MR negative in 1.5 tesla MRI. Until now there have been no systematic comparisons with a higher magnetic field strength of 7 tesla or beyond. The signal to noise ratio is linearly related to the magnetic field strength (23). Thus, a magnetic field strength of 7 tesla could yield more than twice the anatomical resolution and higher detection rates.

Despite high-resolution MRI, post-operative histopathological studies show that up to 50-80% of FCDs

escape visual detection (24). In addition, the limitation of general visibility of structural lesions (technical factors) the human component, i.e. the visual interpretation of MR images, represents a further source of error. In one study preoperative MRI of operated epilepsy patients read as MR-negative was reevaluated after an FCD could be proven histopathologically. Being aware of the fact that there was an FCD, 34% of these FCD could be found in the second round (25). Furthermore, a significant difference in the detection of structural lesions between epileptologically experienced neuroradiologists and those with less expertise in this field (50% *vs.* 39% reported focal lesions) could already be demonstrated (26). This shows that technical advances alone may not be sufficient to improve the detection rates i.e., higher resolution or contrast of MRI are unlikely to proportionally relate to improved visual detection. In this context, the application of automated assessment techniques may be particularly helpful in improving visual detection of lesions. We have reviewed the literature and summarized the available methods of structural post-processing with a focus on individualized diagnostic.

## The methods

### *Voxel-based morphometry (VBM)*

Since the first introduction of VBM at the end of the 1990s, this method has been very frequently used for various neuroscientific questions. Publication counts on PubMed show over the last years an exponential increase of 597 hits when searching “VBM” in 2013. VBM is commonly performed using statistical parametric mapping (SPM), a software package for MATLAB that is freely available. This software is designed for the analysis of brain imaging data sequences and is continuously evolving. For detailed information about this technique we would like to refer to the original publications, describing the principles of VBM (27-30). In brief, the concept of VBM is: for statistical analyses between different individuals the MRI scans need to be matched spatially. The different regions are expanded or contracted to fit a given stereotactic space or template. This template can be created by an average from a large number of MRI scans. The whole process is known as “spatial normalization”. Different algorithms can be used to perform this registration but they typically include a nonlinear transformation. This is not an uncritical process given that a “perfect” spatial normalization would level out all structural differences between individual

brains. To adjust this, a later step called modulation can be applied in which the amount of grey matter is corrected according to the amount of contraction or expansion during spatial normalization, so that the total amount of gray matter remains the same as in the original image. Another important step is segmenting into different tissue compartments [usually gray matter, white matter and cerebrospinal fluid (CSF)] so that each voxel is assigned a probability to belong to a certain tissue class. As a third step, images need to be “smoothed”, a further method to decrease the variance between different brains. The “smoothing” step is, furthermore, necessary to allow data better to conform to the model of Gaussian random fields, which is a basic assumption for most statistical analysis in VBM. The statistical analysis is usually based on a mass-univariate approach (a single test applied repeatedly to all voxels) of these processed probability maps. As this voxel-by-voxel analysis comprises of about 1,400,000 voxels (in 1 mm<sup>3</sup> resolution) and the same number of tests, it is needed to correct the multiple testing problem so to reduce false positive results. Therefore, methods such as the family wise error correction (FWE) (31) or the false discovery rate correction (FDR) (32) are used. Most studies use VBM for assessing grey matter volume. White matter, in principle, can be evaluated in the same way, while different methods as diffusion tensor imaging are usually preferred in white matter.

Several modifications to VBM were applied. For a better understanding of later on mentioned modifications, some of which are explained in more detail. *Figure 1* gives a schematic overview of different VBM processing approaches.

Huppertz *et al.* (33) introduced a fully automated MATLAB script called Morphometric Analysis Programme (MAP) for enhanced visualization of features of FCD and other MCD such as blurred gray-white matter junction. After normalization and segmentation the further post processing differs from the classical VBM. First, voxels with signal intensity between grey and white matter are identified with a histogram analysis of the segmented grey matter and white matter image. In a second step, a binary image is created that represents the distribution of these voxels (1= intensity between grey and white matter, 0= else) and then smoothed with a Gaussian kernel. From the resulting image, the so-call “junction map”, the average of equally processed images of a normal population is subtracted and divided by the standard deviation to create a map of z-scores. By using the same post-processing but applying the grey matter

intensity to create the binary mask the so called “extension” map is calculated. A third map has been described by Huppertz *et al.* and is created by identifying the cortical thickness and comparing this to the normal controls. Voxel-based texture analysis, introduced by Bernasconi *et al.* (34), is a post-processing method that provides quantitative information about spatial gray level variations in pixel neighborhoods, creating maps that highlight cortical thickening, blurring of the grey–white matter junction and relative signal intensity. Colliot *et al.* (35) described an image segmentation approach using deformable models on a level set base in contrast to the parametric base and postulated a better delineation of FCDs.

VBM, as described above, is classically applied to T1-weighted sequences, but can also be applied to other sequences.

Recently, House *et al.* (36) and Braga *et al.* (37) used T2-weighted sequences processed according to the approach of Huppertz *et al.* (33) and described a higher sensitivity for subtle signal intensity differences of FCDs in T2 compared to T1.

VBM based on *T2-FLAIR* is another relatively new application. The advantage of T2-FLAIR is the use of the T2-contrast of FCDs without the afore mentioned problem of high signal intensity of CSF on cortical surface. The high CSF signal does not need to be corrected by post-processing, but can be suppressed at the stage of image acquisition. On the other hand, T2-FLAIR has relatively poor gray/white matter contrast and so the segmentation process may be difficult. Therefore, an additional T1-weighted scan is usually needed to perform a valid segmentation (after co-registration). Recent advances (multi-channel segmentation) allow for a parallel inclusion of T2-FLAIR and T1 so to mutually improve the segmentation quality. As an additional processing step, intensity normalization needs to be included. The following steps as spatial normalization and smoothing are similar to VBM in T1 or T2 enabling a voxel by voxel comparison against a control group (38).

Rugg-Gunn *et al.* (39) applied quantitative voxel-based analysis to MR imaging acquired with double inversion recovery (DIR), which shows advantages when compared to common T1-weighted sequences by minimalizing signal from CSF and white matter so to better visualize the cortical ribbon. DIR is, in some aspects, comparable to FLAIR in T2-weighted sequences but usually suffers from a low signal to noise due to the second inversion pulse.

Magnetization transfer imaging (MTI) is another

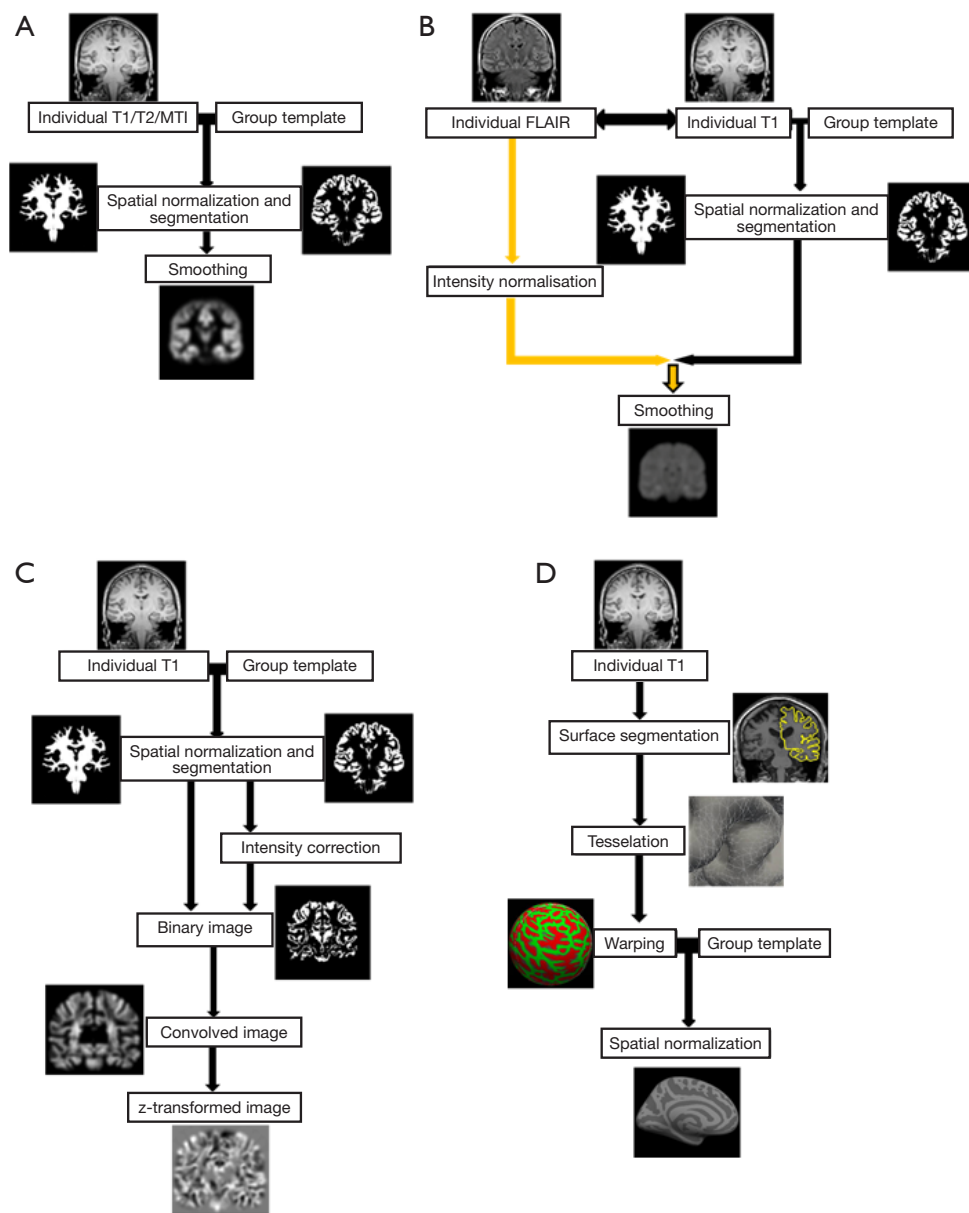


**Figure 1** Schematic overview of different VBM processing approaches. (A) Workflow of a “classical” VBM, e.g., in SPM, based on a T1-weighted image. The individual T1-weighted image is spatially normalized, segmented and smoothed. Similar workflows can be applied for magnetization transfer and T2-weighted images; (B) workflow for normalized T2-FLAIR signal intensity mapping. Segmentation and normalization is performed combined with a T1-weighted and T2-FLAIR image (after co-registered). As an additional processing step, intensity normalization of T2-FLAIR needs to be included. The other steps are similar to (A); (C) workflow following the MAP by Huppertz *et al.*, exemplarily shown with the so called “junction map”. Normalization and segmentation are similar to classical VBM above including bias correction. Next, a binary image is created that represents the distribution of voxels with intensities between grey and white matter and then smoothed (convolved image). From the resulting image, the average of equally processed images of a normal population is subtracted and divided by the standard deviation to create a map of z-scores; (D) workflow of SBM, e.g., using Freesurfer, based on a T1-weighted image. As a first step, the boundaries between the gray/white matter and the pial surface are determined on the basis of a brain segmentation. Then the surfaces are tessellated by polygons whose meeting points or vertexes can be characterized by coordinates. To enable comparison between subjects, the brain images are warped into a common space, usually a sphere. On this basis the brains can be spatially normalized to a given template. VBM, voxel-based morphometry; SPM, statistical parametric mapping; MAP, Morphometric Analysis Programme; SBM, surface-based morphometry.

sequence that can be evaluated as a voxel-based post-processing method. MTI indirectly gives information about the content of macromolecules and thus, can indicate microstructural damage (40). The most common application of MT imaging in neurology is the detection of lesions in multiple sclerosis. Some studies have adopted this method for the detection of subtle cortical lesions.

### *Surface-based morphometry (SBM)*

SBM refers to a group of techniques that reconstruct and analyze the cortical surface of the brain respecting the individual highly folded geometry. It tries to complement potential gaps of VBM in detecting spatially restricted lesions which are hidden in the gyrification of the brain. After removing extracerebral voxels with a process called skull-stripping, the boundaries between the gray/white matter and the pial surface are determined on the basis of a brain segmentation and usually using intensity levels of voxels, similar to the VBM-approach. Then the surface of the cortex and the gray/white matter junction is tessellated by polygons whose meeting points or vertexes can be characterized by coordinates in the x, y and z plane. With these coordinates, further image processing such as unfolding and flattening of the surface can be performed. In order to compare these parameters with a group of controls, the brain images have to be spatially normalized similar to VBM. For this alignment, the surface is flattened by “blowing up” the brain into a parameterizable surface, usually a sphere to establish a surface-based coordinate system, which is comparable among different subjects. After matching the size of a subject’s sphere to a control group, statistical analysis can be performed e.g., to quantify differences in cortical thickness, the rate of curvature, grey/white-contrast or a gyrification index. For further information, please refer to more detailed publications (41–43). The commonly used software for SBM applications is Freesurfer (free software for analyzing brain MRI images). Further software packages are available such as BrainVoyager (commercial neuroimaging tool).

While SBM enjoys great popularity in other pathological entities such as autism or schizophrenia, there are currently only rare applications in epilepsy. Blackmon *et al.* (44) introduced an approach for assessing the blurring of the grey/white matter junction as a feature of FCDs by calculating the non-normalized T1 image intensity contrast at 0.5 mm above versus below the grey/white matter junction. Resulting values ranged from –1 to 0, with values

closer to zero indicating a higher degree of blurring at the grey-white matter boarder.

### *MR-relaxometry*

Relaxometry describes the quantitative measurement of relaxation times in the brain (usually T1 and/or T2). Being objective and absolute, this method may be particularly helpful in recognizing subtle changes. Acquiring accurate T1 and T2 maps, however, requires longer and more dedicated acquisition paradigms such as double angle methods (for T1) or multiple echo-time spin-echo sequences (for T2). Due to long acquisition times, these methods remain reserved in clinical diagnostic to special questions; in epileptology T2 relaxometry is routinely applied in temporal lobe epilepsy and hippocampus sclerosis. Mostly, a regional analysis of the average values per slice (e.g., of the hippocampus) is done. An alternative approach uses a histogram of relaxation values. Signal alterations will show a shift in the distribution of a predefined region of interest compared to a control group. This approach is intuitive and needs no structural normalization, just a normalization of the numbers of voxels included in the compared areas. Depending on the size of the selected region of interest, the spatial resolution of this approach is limited (45–47).

For a full-brain approach, relaxation times can be compared voxel by voxel as “voxel-based relaxometry”, which means that processing steps of spatial normalization and smoothing are necessary (48).

A problem in all T2-weighted sequences is the high signal of CSF which imposes a partial-volume problem especially on cortical surface and necessitates masking further mathematical masking techniques.

### *Diffusion tensor imaging*

Detailed information on DTI are available (49–51) and in a separate article in this issue.

In brief, DTI estimates a diffusion tensor based on the fact that the diffusion of water molecules differs depending on structural conditions. Most common measures are the trace (sum of the diagonal elements) and anisotropy of the diffusion tensor. The latter is usually simplified further by quantifying anisotropy with values between 0 (= isotropy) and 1 (= all diffusion along one direction), called fractional anisotropy. Further dimensions such as tensor orientation or axial and radial diffusivity are less commonly applied. For voxel-wise comparison to a control group post-processing

steps include spatial normalization as well as smoothing, similar to VBM. An alternative approach projects DTI values on a common pseudo-anatomical skeleton representing the centres of all fibre tracks that are generally common to the subjects involved (52). This approach (TBSS) can reduce the multiple comparison problem and yield improved statistical power (53).

Winston *et al.* (54) recently evaluated an advancement of DTI called NODDI in epilepsy which adds additional estimates of tissue microstructure in both grey and white matter by assessing the neurite density and fibre orientation dispersion.

Besides the above mentioned studies, DTI is commonly applied for preoperative visualization of important tracts such as the corticospinal tract to assess possible interfering with the planned resection zone of a FCD.

## Results

We have reviewed the Medline database (15.10.2014, Keywords: “epilepsy, voxel based”; “epilepsy, relaxometry”; “epilepsy, magnetization transfer imaging”; “epilepsy, diffusion tensor imaging”; “epilepsy, surface based”; “focal cortical dysplasia, epilepsy, quantitative”) and identified 35 studies relevant to the post-processing for individual diagnostics. Of these 12 applied T1-based VBM, 1 T2-based VBM, 4 FLAIR-based VBM, 2 DIR-based VBM, 3 SBM, 7 MR-relaxometry, 3 voxel-based texture analysis, 1 level set method. Details are shown in *Table 1*.

Not all studies listed in *Table 1* applied their method(s) to visually MRI negative patients in cryptogenic epilepsy as an indicator for their additional value in clinical diagnostics. One major problem of the available studies is that not every detected lesion can be confirmed as epileptogenic since histopathological confirmations and outcome data are not commonly available or electroclinical findings are inclusive. For this reason, detected lesions by post-processing analysis (PPA) are quantified in a “detection rate” [ $n$  (detected lesion)/ $n$  (total) = ratio] and lesions with correct correlation to histopathology exceeding detection in conventional visual analysis are quantified as “diagnostic yield” = [ $n$  (diagnosed lesion)/ $n$  (total)]. Studies on cryptogenic epilepsy have a different approach and cannot be compared evenhandedly to retrospective studies with already histopathologically proven FCDs. For this reason, we decided to indicate detected lesions by post-processing methods in cryptogenic epilepsy in a separate way. Detected lesions in cryptogenic epilepsy with a correct correlation to electroclinical findings

are quantified as “detection yield” = [ $n$  (detected lesions)/ $n$  (total)]. Positive findings from conventional visual analysis in studies without histopathological confirmation were subtracted from  $n$  (total) to better objectify the true benefit of a distinct processing method in cryptogenic epilepsy.

### *Post-processing in patients with known lesions*

VBM, using T1-weighted sequences, detected 38-95% (37,55) of all lesions identified by conventional visual analysis. The study from Riney *et al.* (55) with only 38% detected lesions is an outlier, most other studies detecting over 60% of lesions (56-60). Studies on T1-weighted sequences using the Morphometric Analysis Programme (MAP) introduced by Huppertz *et al.* (33) reported detection rates between 88-100% (33,36,61,62). House *et al.* (36) also applied MAP in T2-weighted sequences and showed an equally high detection rate with 100% and reported a visually better contrast and/or clearer delineation in 80% of lesions as well as higher z-scores in 95% of cases. VBM of FLAIR resulted in 88-97% (38,55,63) (last one in hippocampal sclerosis) matched detected lesions. The application of VBM in DIR yielded in one study a concordance of 100% (39).

T2-relaxometry yielded a concordance with conventional visual analysis of 100% in the four studies in temporal lobe epilepsy (48,64-66).

For diffusion imaging, Eriksson *et al.* (67) (for voxel-based analysis of DTI), and recently Winston *et al.* (54) (for an advanced DTI processing called NODDI) showed a correspondence with conventional visual analysis in 68% and 100% respectively (in the latter only in a small cohort of five subjects as an introduction of a new method). The approach of SBM achieved 91% and 100% (44,68) concordant detections in two recent studies. However, Thesen *et al.* (68) noted that the method failed to capture the extension of the lesions sufficiently. The second study included an additional feature of quantifying blurring of the grey/white matter junction. VBM based on MTI could identify 87% and 100% of the visually detected MCDs (69,70). Texture analysis was introduced by Bernasconi *et al.* (34) and was later expanded with additional surface features described by Besson *et al.* (24), reporting detection rates of FCDs of 100% and 95%. One attempt using level set evolution by Colliot *et al.* (35) detected 75% of the conventionally visible FCDs.

Overall, the vast majority of MR-visible lesions can also be detected by automated post-processing methods. This

**Table 1** Studies on MRI post-processing methods in epilepsy on an individual basis, ordered by method and year

Method	Author	Year	n	Ref.	CVA [%]	PPA-detection rate [%]	Concordance of CVA and PPA [%]	PPA detected lesions exceeding CVA (diagnostic yield or detection yield) [%]
VBM T1 (MAP-extension image only)	Kassubek J, et al.	2002	7	im†	7/7 [100]	6/7 [100]	7/7 [100]	-
VBM T1 (MAP)	Huppertz HJ, et al.	2005	25	hi§	21/25 [84]	21/25+ [84]	17/21 [81]	4/25 [16]
	Wagner J, et al.	2011	91	hi	78/91 [86]	82/91+ [90]	69/78 [88]	13/91 [14]
VBM T1 + T2 (MAP)	House PM, et al.	2013	20	im	20/20 [100]	20/20 [100] in T1 and T2	20/20 [100]	-
VBM T1 (MAP)	Wang ZI, et al.	2014	25	ec†/hi	0/25 [0]	12/25 [48]	-	12/25 [48]
VBM T1	Wilke M, et al.	2003	20	im/hi	20/20 [100]	19/20 [95]	19/20 [95]	-
	Colliot O, et al.	2006	27	im	27/27 [100]	21/27 [78]	21/27 [78]	-
	Bonilha L, et al.	2006	11	im/hi	11/11 [100]	10/11 [91]	10/11 [91]	-
	Salmenpera TM, et al.	2007	93	ec	0/93 [0]	7/75 [9]-rest data processing failed	-	7/75 [9]
	Bruggemann JM, et al.	2009	8	im	8/8 [100]	5/8 [62.5]	5/8 [62.5]	-
	Pail M, et al.	2012	18	im/ec	10/18 [56]	13/18 [72]	10/10 [100]	3/8 MRI- [38]
VBM FLAIR	Focke NK, et al.	2008	25	im	25/25 [100]	22/25 [88]	22/25 [88]	-
	Focke NK, et al.	2009	70	ec	0/70 [0]	8/70 [11]	-	8/70 [11]
	Huppertz HJ, et al.	2011	103	im	103/103 [100]	100/103 [97]	100/103 [97]	-
VBM FLAIR + T1	Riney CJ, et al.	2012	22	im/ec	8/22	9/22 FLAIR [41], 3/22 T1 [14]	7/8 FLAIR [88], 3/8 T1 [38]	2/14 MRI-FLAIR [14], 0/14 MRI-T1 [0]
Level set method	Colliot O, et al.	2006	24	im	24/24 [100]	18/24 [75]	18/24 [75]	-
Voxel-based analysis DIR	Rugg-Gunn FJ, et al.	2006	47	im/ec	14/47 [30]	24/47 [51]	14/14 MRI+ [100]	10/33 MRI- [30]
	Salmenpera TM, et al.	2007	93	ec	0/93 [0]	13/83 [16]-rest data processing failed	-	13/83 [16]
SBM	Thesen T, et al.	2011	11	im	11/11 [100]	10/11 [91]	10/11 [91]	-
	Hong SJ, et al.	2014	15	hi	0/15 [0]	10/15 [67]	-	10/15 [67]
	Blackmon K, et al.	2014	20	hi	6/20 [30]	20/20 [100]	6/6 MRI+ [100]	14/20 [70]

**Table 1** (continued)

Table 1 (continued)

Method	Author	Year	n	Ref.	CVA [%]	PPA-detection rate [%]	Concordance of CVA and PPA [%]	PPA detected lesions exceeding CVA (diagnostic yield or detection yield) [%]
Voxel-based T2-relaxometry	Bernasconi A, et al.	2000	25	im/ec	14/25 [56]	23/25 [92]	14/14 [100]	9/11 [82]
	Pell GS, et al.	2004	19	im	19/19 [100]	19/19 [100]	19/19 [100]	-
	Rugg-Gunn FJ, et al.	2005	65	im/ec	20/65 [31]	18/20 MRI+ [90]; 23/45 MRI- [51]	18/20 MRI+ [90]	20/45 MRI- [51]
ROI T2-relaxometry	Bartlett PA, et al.	2007	20	im	20/20 [100]	20/20 [100]	20/20 [100]	-
Voxel-based FFT2-relaxometry	Salmenpera TM, et al.	2007	93	ec	0/93 [0]	13/82 [16]-rest motion artifacts	-	13/82 [16]
VBIS relaxometry	Abbot DF, et al.	2009	24	im	24/24 [100]	24/24 [100]	24/24 [100]	-
Voxel-based T2-relaxometry	Kosior RK	2012	59	im/ec	27 questionably MRI+, 32 MRI-	22/32 MRI- [69]; 24/27 questionably MRI+ [89]	19/27 questionably MRI+ [70]	16/32 [50]
Voxel-based analysis DTI	Eriksson SH, et al.	2001	22	im	22/22 [100]	18/22 [82]	15/22 [68]	-
	Rugg-Gunn FJ, et al.	2001	30	ec	0/30 [0]	8/30 [27]	-	7/30 [23]
	Rugg-Gunn FJ, et al.	2002	1	ec	0/1 [0]	1/1 [100]	-	1/1 [100]
NODDI	Winston GP, et al.	2014	5	im	5/5 [100]	5/5 [100]	5/5 [100]	-
MTI voxel based analysis	Rugg-Gunn FJ, et al.	2003	57	im/ec	15/57 [26]	13/15 MRI+ [87]; 15/42 MRI-	13/15 MRI+ [87]	15/42 MRI- [36]
	Salmenpera TM, et al.	2007	93	ec	0/93 [0]	4/77 [5]-rest motion artifacts	-	4/77 [5]
	Kadom N, et al.	2013	7	im	7/7 [100]	7/7 [100]	7/7 [100]	-
Voxel-based texture analysis	Bernasconi A, et al.	2001	16	hi	8/16 [50]	14/16 [88]	8/8 MRI+ [100]	6/16 [38]
	Colliot O, et al.	2006	23	hi	16/23 [76]	23/23 [100]	16/16 [100]	7/23 [30]
Surface-based texture analysis	Besson P, et al.	2008	19	im	19/19 [100]	18/19 [95]	18/19 [95]	-

Table 1 lists all studies considered in this review ordered by method and year. It indicates the number of detected lesions by conventional visual analysis (CVA) compared to the lesions detected by the particular post-processing analysis (PPA) = detection rate = [n (detected lesion)/n (total)]. Furthermore, concordance between CVA and PPA detected lesions is shown to give an impression of the diagnostic power of automated post-processing methods compared to conventionally detected lesions. Detected lesions with correct correlation to histopathology exceeding detection in conventional visual analysis are quantified as diagnostic yield = [n (diagnosed lesions)/n (total)]. Detected lesions in cryptogenic epilepsy with a correct correlation to electroclinical findings are quantified as detection yield = [n (detected lesions)/n (total)]. Positive findings from conventional visual analysis in studies without histopathological confirmation were subtracted from n (total) to objectify better the benefit of a distinct method in cryptogenic epilepsy. Ratios are rounded to integers. N, number of patients; <sup>†</sup>im, imaging; <sup>‡</sup>ec, electroclinical; <sup>§</sup>hi, histopathology. VBM, voxel-based morphometry; CVA, conventional visual analysis; PPA, post-processing analysis; MAP, Morphometric Analysis Programme; DIR, double inversion recovery; SBM, surface-based morphometry.

is not very surprising since all methods are usually tested against and trained based on the available standard of care (visual reading) and a method not capable of detecting at least the majority of visible lesions will usually not be published. It is currently unclear which method and which underlying sequence is preferable, given the lack of studies directly comparing the different approaches.

### **Detection of lesions in cryptogenic epilepsy**

For T1-weighted VBM, Pail *et al.* (60) detected lesions in 4 patients from a cohort of 18 children with temporal lobe epilepsy in addition to the 10 already MRI positive subjects, from whom 3 corresponded to histopathological findings after resection (diagnostic yield of 3/8 =38%). This study used DARTEL normalization as a relatively new feature in SPM. In contrast, Riney *et al.* (55) did not succeed in detecting any lesion in their cohort of 14 MRI negative children, that corresponded to electroclinical expectations (2/14, none concordant). In the same cohort, FLAIR based VBM was able to detect 4/14 suspect lesions, of whom 2 corresponded to the electroclinical results (detection yield 2/14 =14%). Focke *et al.* (71) applied FLAIR based VBM in 70 MRI negative patients. In eight subjects VBM demonstrated new findings that were concordant to the electro-clinical results (detection yield 8/70 =11%). A validation with histopathological findings after surgery was not available for both studies.

Wagner *et al.* (62) took a different approach and correlated VBM findings to histopathological results in 91 patients with post-operatively detected FCDs. Using MAP they correctly detected 5/6 FCD IIa and 6/7 FCD IIb that were missed in conventional, visual MRI analysis (diagnostic yield of FCD IIa 5/17 =29%; FCD IIb 7/74 =9%). Huppertz *et al.* (33) succeeded in detecting four FCDs more than conventional visual analysis in a cohort of 25 histopathologically proven FCDs (diagnostic yield 4/25 =16%).

In the study by Rugg-Gunn *et al.* (39) using DIR and voxel-based analysis, 10-15 lesions out of 33 MRI-negative patients could be detected [detection rate 15/33 (45%); detection yield 10/33 (30%)]. There were no histopathological correlations, but at least ten lesions were in keeping with the electroclinical findings.

Three studies applied T2-relaxometry in cryptogenic epilepsy. Focusing on temporal lobe epilepsy, Bernasconi *et al.* (65) demonstrated a detection of nine patients with formerly missed lesions in the temporal lobe in a collective of

11 MRI-subjects (detection yield 9/11 =82%). Seven MRI-negative patients underwent surgery, and histopathological findings showed structural alterations in form of gliosis and neuronal loss in 5. Rugg-Gunn *et al.* (72) applied T2-relaxometry for the whole brain and were able to detect 20 potential epileptogenic lesions in their cohort of 45 patients that matched the localization of epileptic video-EEG abnormalities (detection yield 20/45 =51%), histopathological correlations were not available. Kosior *et al.* (73) identified 22/32 abnormalities (detection rate 22/32 =69%), from whom 16/32 corroborated electro clinical findings (detection yield 50%). Yet they chose a low statistical threshold at the expense of specificity and false positive findings.

One study with 30 MRI-negative patients and one case report by Rugg-Gunn *et al.* (74,75) showed the additional usefulness of diffusion imaging in cryptogenic epilepsy. Seven out of 30 MRI-negative patients were shown to have a lesion concordant with video-EEG findings (detection yield 7/30 =23%). Derived from this work, one case report describes the successful operation (improvement of seizures, Engel Class IIa) of a lesion in the orbitofrontal cortex based on EEG and diffusion tensor imaging with the histopathological confirmation in form of diffuse gliosis in the resected area.

The recently published approach of SBM by Blackmon *et al.* (44) correlated SBM findings to histopathological results in 20 patients with post-operatively detected FCDs, where conventional visual analysis only succeeded in 6/20. They were able to identify 20/20 FCD (diagnostic yield 14/20 =70%). Hong *et al.* detected in a retrospective study 10 corroborating lesions out of 15 histologically proven, MRI-negative FCDs (diagnostic yield =67%).

The use of MTI in cryptogenic epilepsy was shown in one study (69) with 15/42 detected lesions of previously MRI-negative patients concordant with video-EEG (detection yield 15/42 =36%), but without further histopathological correlation.

Two studies on voxel-based texture analysis (34,76) could detect more FCDs than conventional visual analysis. The first study detected 6 lesions more (detection yield 6/16 =38%), the second 7 (diagnostic yield 7/23 =30%).

In conclusion, all of the above mentioned methods are able to detect a certain amount of lesions that escape conventional visual detection. The detection/diagnostic rate highly varies among the studies, even when applying the same method. In retrospective studies of histopathologically proven lesions, diagnostic rates are, as expected, much higher than in prospective studies on unselected pharmaco-

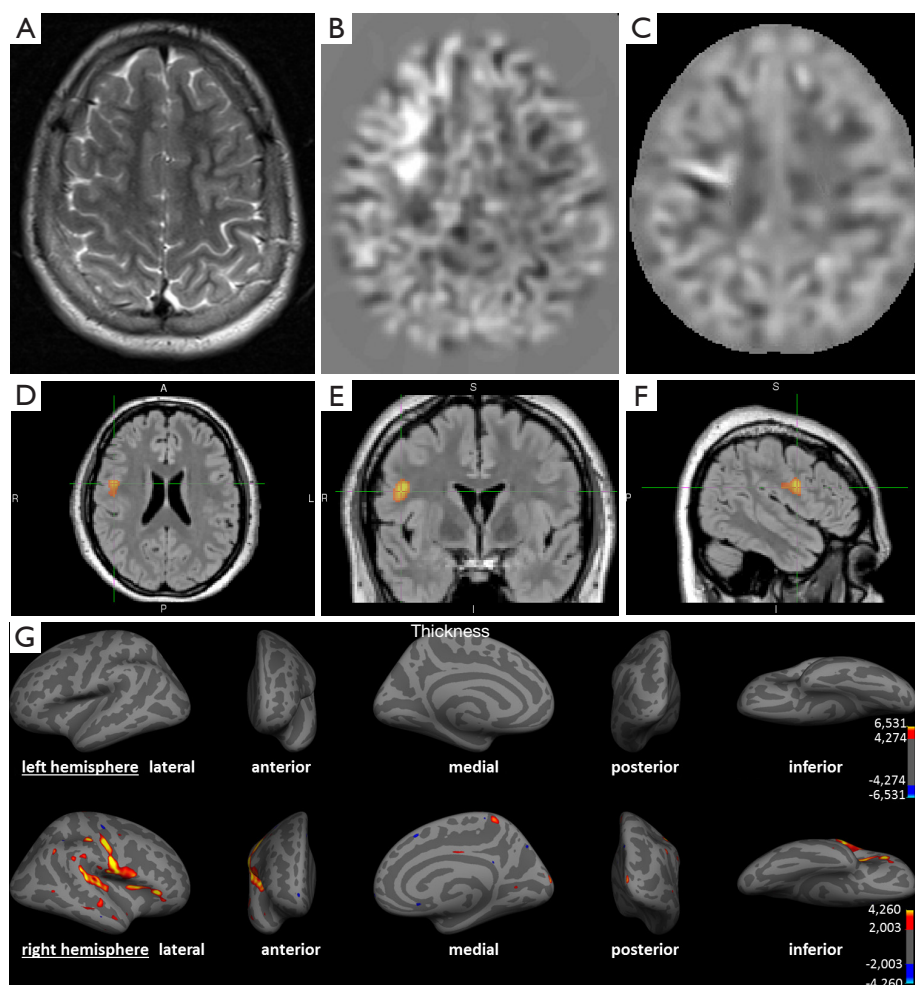


**Figure 2** A 14-year-old child with partial (clonuses of the left hand and leg) and secondary generalized seizures since the age of 4. (A) Axial T2-weighted image; (B) axial calculated junction map (window setting  $-4$  to  $+4$  z-score) based on a T1 MPRAGE sequence; (C) axial calculated extension map (window setting  $-7$  to  $+7$  z-score) based on a T1 MPRAGE sequence; (D-F) voxel-based morphometry of FLAIR, using SPM in axial, coronal and sagittal view; (G) SBM using Freesurfer representing left (upper row) and right (lower row) hemisphere. (A) No detectable structural lesion in conventional visual analysis; (B) brighter clusters in the junction map indicating blurring of the grey-white matter junction e.g., due to a focal cortical dysplasia; (C) brighter clusters in the extension map indicating abnormal extension of grey matter into white matter e.g., abnormal gyration; (D-F) colored clusters represent regions with significantly increased FLAIR intensities ( $P < 0.05$  FWE corrected); (G) colored vertices show significant increased cortical thickness ( $P < 0.05$  FDR corrected) compatible to an MCD. All post-processing methods indicate converging the presence of a lesion in the right frontal and insular cortex. The findings in post-processing methods were congruent with EEG findings. Based on these results the patient was operated, histopathology showed a focal cortical dysplasia type IIa. The patient benefited from the operation in form of a reduction of seizure frequency and intensity. SPM, statistical parametric mapping; SBM, surface-based morphometry; FWE, family wise error correction; FDR, false discovery rate correction; MCD, malformations of cortical development.

resistant, pre-surgical populations. Different cohort size, different tolerated false positive findings in the control group, preselected subjects or the absence of a gold standard are just some of the problems that impede cross

comparison. In addition, MR-technological advances developed in parallel to post-processing methods and may have improved conventional visual analysis.

*Figure 2* shows the detection of a FCD in post-processing

that has not been detected on the initial conventional visual analysis.

### *Comparison of the different post-processing methods*

Only a few studies apply more than one post-processing method to the same cohort of patients enabling direct comparisons. Riney *et al.* (55) compared VBM of T1-weighted sequences with VBM of FLAIR and report higher detection rates of FLAIR compared to T1 in detection of MRI-positive and MRI-negative lesions [7/8 MRI+ in FLAIR (88%), 3/8 MRI+ in T1 (38%); 2/14 MRI- in FLAIR (14%); 0/14 MRI- in T1]. House *et al.* (36) compared T1- and T2-weighted sequences in MAP in a cohort of 20 MRI-positive subjects. Both approaches detected all lesions, but T2 was superior in showing better visual contrast of the detected lesions in 80%, only one had a more favorable contrast in T1.

Finally, Salmenpera *et al.* (77) compared four post-processing methods (voxel-based fast FLAIR T2-relaxometry, VBM T1, voxel-based analysis of DIR, voxel-based analysis of MTI) in the same cohort of 93 MRI-negative patients with FE and compared these with the results of video-EEG telemetry. Voxel-based DIR and voxel-based FFT2-relaxometry succeeded both in detecting 13 lesions (detection yield 13/82 respectively 13/83 =16%). VBM in T1 found 7 concordant lesions (detection yield 7/75 =9%), while voxel-based analysis of MTI detected 4 (detection yield 4/77 =5%).

A total of 34 of these detected lesions in patients could be correspondingly detected (defined as in the same lobe) in at least two contrasts, while most frequent colocalization was found between FFT2 and DIR (27 patients, 31%). Seven patients (9%) showed colocalization in at least 3 contrasts, most frequently between FFT2, DIR, and VBM (6 patients, 8%). Three patients (4%) had a concurring abnormality for all 4 post-processing methods. Restricting concurrence from correct hemisphere to correct lobe, the number of correct detections reduced in total to 26 patients (31%).

A correlation with histopathological findings was possible in 5 operated patients. Four of them showed a detected lesion in post-processing methods correlating to the operated area. Three of these 4 experienced an improvement of their seizures. Histopathology showed defined lesions (hippocampal sclerosis, hamartoma, FCD), while in the other two cases gliosis and atrophy.

The study by Salmenpera *et al.* (77) demonstrated not only the ability of detecting lesions that were missed on

conventional visual analysis. A detection rate of overall 30% faces 36% FFT2 signal changes outside the lobe of the putative focus and 42% in DIR. Kosior *et al.* (73) detected at least one abnormality in 46 of their 59 patients (79%), but also 24 of their 45 control subjects (53%) showed abnormalities. This relatively high rate of false-positive findings may be justifiable in terms of visualizing a potential lesion and thus initiate further focused diagnostics as invasive EEG-monitoring, but it highlights the low specificity in some methods. There is no common statistical threshold in the studies applying automated post-processing methods and this contributes to the range of detected lesion. The need for correlation with clinical findings and additional diagnostic tools as (video-) EEG for verification of the epileptogenicity of a lesion persists even in clearly visible lesions before surgery. Individual diagnostics differs in this aspect from group studies with scientific background, in which false positive findings need to be minimized. *Figure 3* shows an example for an irrelevant finding concerning the epileptological aspect, and a true positive finding.

### **Conclusions**

Post-processing methods in epilepsy pre-surgical evaluation have shown a continuous development since their first scientific introduction in the late 1980s and are valuable tools in routine diagnostic. However, the evidence base of these methods is limited and no study would fulfill strict criteria for level 1 evidence. The majority are retrospective, only partially controlled and are often based on selected cohorts. Thus, the true diagnostic yield compared to conventional visual analysis is difficult to assess using the existing data. It is also likely that it will also be influenced by the quality of visual reading that can vary considerable. Also, only a few studies applied more than one post-processing method in the same cohort of patients, so an objective comparison and assessment of inter-method superiority is very limited.

All methods showed a good concordance to conventional visual analysis, indicating that post-processing may be a screening tool to increase the confidence that no visible lesion was overlooked. This may be particularly important in the era of increasing magnetic field strength (7, 9.4 T and beyond) and increasing image resolution. For most methods, studies could also show the ability to detect epileptogenic lesions that were missed or not visible in conventional visual analysis. This yield of detection ranges from 5-10% and goes up to 70% in retrospective studies

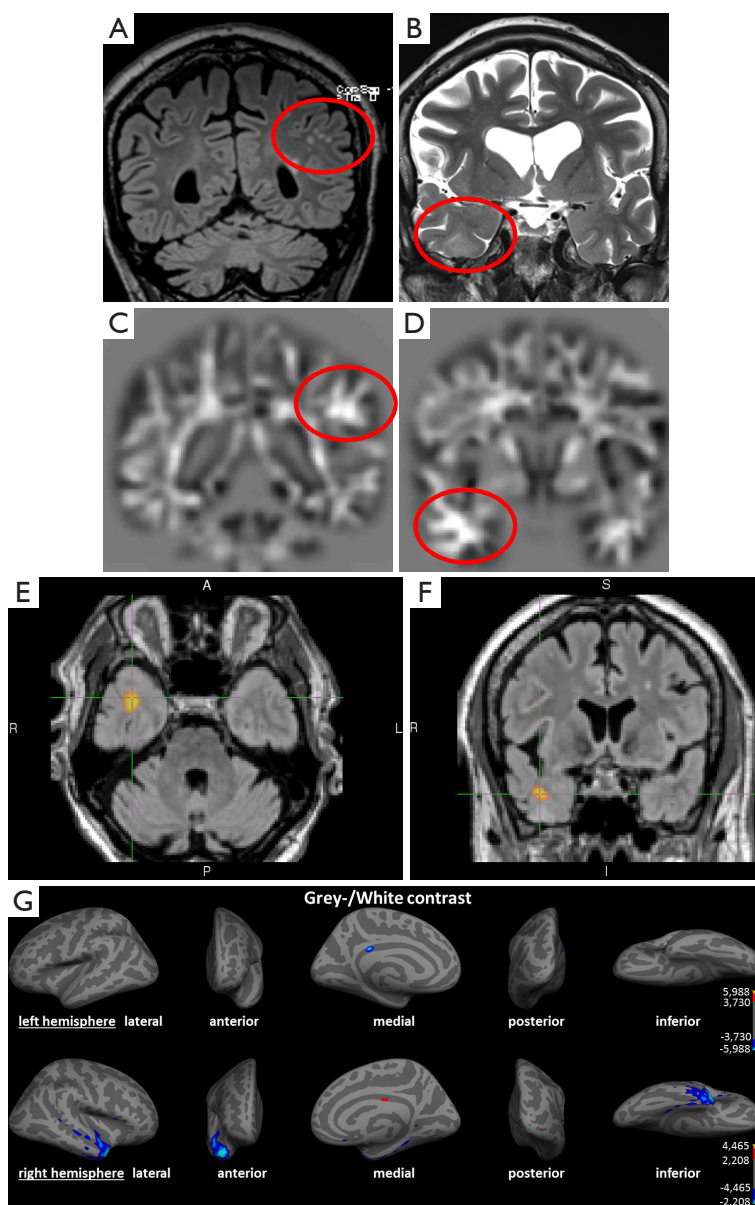


**Figure 3** Example of an irrelevant finding concerning the epileptological aspect and a true positive finding in a 69-year-old patient with partial seizures since the age of 12 and secondary generalized seizures since the age of 40. (A) Coronal FLAIR image; (B) coronal T2-weighted image; (C,D) coronal calculated junction map based on a T1 MPRAGE sequence; (D,E) voxel-based morphometry of FLAIR, using SPM in axial and coronal view; (G) surface-based morphometry using Freesurfer presenting left (upper row) and right (lower row) hemisphere. (A) Structural lesions due to microangiopathy in subcortical white matter (circle); (B) subtle structural changes in the right temporal lobe with blurring of the grey/white matter junction and increased signal intensity (circle); (C) brighter clusters in the junction map indicating blurring of the grey-white matter junction as often seen in a focal cortical dysplasia, yet in this case due to juxtacortical microangiopathy (false-positive); (D) Z-score increase in the junction map indicating a blurring of the grey-white matter junction concordant to conventional visual analysis in (B); (E,F) suprathreshold cluster representing voxels with significantly increase FLAIR intensities indicating structural lesion ( $P < 0.05$  FWE corrected); (G) colored vertices show significant decreased grey/white contrast ( $P < 0.05$  FDR corrected) compatible to an MCD. Correlation with (video-) EEG findings shows the epileptogenic region in the right temporal lobe. The left-sided juxtacortical white matter lesions are to be evaluated as false positive finding. This shows the importance of correlation with other diagnostic features and the advantage of multimodal post-processing. SPM, statistical parametric mapping; FWE, family wise error correction; FDR, false discovery rate correction; MCD, malformations of cortical development.

with selected patients.

On the other hand, conventional visual analysis has been shown to detect lesions that were missed by post-processing in 3-35%. Thus, expert visual analysis and post-processing are complementary diagnostic tools and should be used in conjunction. The influence on the postoperative outcome of surgery of prediction of the lesion in post-processing methods and/or conventional visual analysis is not yet clear. Wagner *et al.* (62) showed no significant difference in the outcome of patients with positive MRI in conventional visual analysis and/or in MAP.

Wang *et al.* (78) could show a higher rate of seizure freedom in MRI-negative patients if the complete lesional area detected by MAP was resected ( $P=0.02$ ).

All automated methods suffer from false positive findings depending on method immanent parameters. Salmenpera *et al.* (77) reported a detection rate of over 30% in MRI-negative patients, but also reported a low specificity with 36% FFT2 signal changes outside the lobe of the putative focus and as much as 42% probably false-positive findings in DIR. Although some of these findings may be network effects or dual pathologies, it is very likely that the majority is spurious. Another way to estimate the specificity of the processing methods is to apply the same method in single cases of healthy controls and regard all “positive” findings as “false-positives”. This approach has been taken by some studies and has many advantages since it can be done in large cohorts and is objective. However, the clinical interest is not to study variations of brain morphometry in healthy but to study epilepsy patients. The true negative control would be patients without lesions, but these are almost impossible to get since even a negative histology after resection does not exclude lesions elsewhere in the brain. Thus, the problem of false-positives remains a very relevant, unsolved issue that all users of post-processing need to be aware about and that requires expertise in interpreting these findings in the context of the multi-disciplinary consensus to reduce the frequency of false positive and false negative findings which inevitably occur (27,79). For this reason these methods should stay reserved, at present, to specialized clinical epilepsy centers.

For the future, further studies comparing several post-processing methods in the same patients with correlation to histopathological findings and clinical outcome would be very desirable. The introduction of even higher MR-field strength (7 tesla and higher) promises a further improvement of anatomical resolution and may result in a higher detection rate. But also software algorithms

(normalization, segmentation) underlie a constant development. Moreover, the combination of several modalities i.e., fMRI, EEG and PET could have a positive impact on the detection of epileptogenic lesions.

*Disclosure:* The authors declare no conflict of interest.

## References

1. Guerrini R, Sicca F, Parmeggiani L. Epilepsy and malformations of the cerebral cortex. *Epileptic Disord* 2003;5 Suppl 2:S9-26.
2. Kabat J, Król P. Focal cortical dysplasia - review. *Pol J Radiol* 2012;77:35-43.
3. Seifer G, Blenkman A, Princich JP, Consalvo D, Papayannis C, Muravchik C, Kochen S. Noninvasive approach to focal cortical dysplasias: clinical, EEG, and neuroimaging features. *Epilepsy Res Treat* 2012;2012:736784.
4. Cotter D, Honavar M, Lovestone S, Raymond L, Kerwin R, Anderton B, Everall I. Disturbance of Notch-1 and Wnt signalling proteins in neuroglial balloon cells and abnormal large neurons in focal cortical dysplasia in human cortex. *Acta Neuropathol* 1999;98:465-72.
5. Blümcke I, Thom M, Aronica E, Armstrong DD, Vinters HV, Palmini A, Jacques TS, Avanzini G, Barkovich AJ, Battaglia G, Becker A, Cepeda C, Cendes F, Colombo N, Crino P, Cross JH, Delalande O, Dubeau F, Duncan J, Guerrini R, Kahane P, Mathern G, Najm I, Ozkara C, Raybaud C, Represa A, Roper SN, Salamon N, Schulze-Bonhage A, Tassi L, Vezzani A, Spreafico R. The clinicopathologic spectrum of focal cortical dysplasias: a consensus classification proposed by an ad hoc Task Force of the ILAE Diagnostic Methods Commission. *Epilepsia* 2011;52:158-74.
6. Avoli M, Louvel J, Mattia D, Olivier A, Esposito V, Pumain R, D'Antuono M. Epileptiform synchronization in the human dysplastic cortex. *Epileptic Disord* 2003;5 Suppl 2:S45-50.
7. Bast T, Oezkan O, Rona S, Stippich C, Seitz A, Rupp A, Fauser S, Zentner J, Rating D, Scherg M. EEG and MEG source analysis of single and averaged interictal spikes reveals intrinsic epileptogenicity in focal cortical dysplasia. *Epilepsia* 2004;45:621-31.
8. Leventer RJ, Phelan EM, Coleman LT, Kean MJ, Jackson GD, Harvey AS. Clinical and imaging features of cortical malformations in childhood. *Neurology* 1999;53:715-22.
9. Yao K, Mei X, Liu X, Duan Z, Liu C, Bian Y, Ma Z,

- Qi X. Clinical characteristics, pathological features and surgical outcomes of focal cortical dysplasia (FCD) type II: correlation with pathological subtypes. *Neurol Sci* 2014;35:1519-26.
10. Fauser S, Schulze-Bonhage A, Honegger J, Carmona H, Huppertz HJ, Pantazis G, Rona S, Bast T, Strobl K, Steinhoff BJ, Korinthenberg R, Rating D, Volk B, Zentner J. Focal cortical dysplasias: surgical outcome in 67 patients in relation to histological subtypes and dual pathology. *Brain* 2004;127:2406-18.
  11. Colombo N, Tassi L, Galli C, Citterio A, Lo Russo G, Scialfa G, Spreafico R. Focal cortical dysplasias: MR imaging, histopathologic, and clinical correlations in surgically treated patients with epilepsy. *AJNR Am J Neuroradiol* 2003;24:724-33.
  12. Krsek P, Maton B, Korman B, Pacheco-Jacome E, Jayakar P, Dunoyer C, Rey G, Morrison G, Ragheb J, Vinters HV, Resnick T, Duchowny M. Different features of histopathological subtypes of pediatric focal cortical dysplasia. *Ann Neurol* 2008;63:758-69.
  13. Kim YH, Kang HC, Kim DS, Kim SH, Shim KW, Kim HD, Lee JS. Neuroimaging in identifying focal cortical dysplasia and prognostic factors in pediatric and adolescent epilepsy surgery. *Epilepsia* 2011;52:722-7.
  14. Lerner JT, Salamon N, Hauptman JS, Velasco TR, Hemb M, Wu JY, Sankar R, Donald Shields W, Engel J Jr, Fried I, Cepeda C, Andre VM, Levine MS, Miyata H, Yong WH, Vinters HV, Mathern GW. Assessment and surgical outcomes for mild type I and severe type II cortical dysplasia: a critical review and the UCLA experience. *Epilepsia* 2009;50:1310-35.
  15. Seo JH, Holland K, Rose D, Rozhkov L, Fujiwara H, Byars A, Arthur T, DeGrauw T, Leach JL, Gelfand MJ, Miles L, Mangano FT, Horn P, Lee KH. Multimodality imaging in the surgical treatment of children with nonlesional epilepsy. *Neurology* 2011;76:41-8.
  16. Téllez-Zenteno JF, Hernández Ronquillo L, Moien-Afshari F, Wiebe S. Surgical outcomes in lesional and non-lesional epilepsy: a systematic review and meta-analysis. *Epilepsy Res* 2010;89:310-8.
  17. Colombo N, Citterio A, Galli C, Tassi L, Lo Russo G, Scialfa G, Spreafico R. Neuroimaging of focal cortical dysplasia: neuropathological correlations. *Epileptic Disord* 2003;5 Suppl 2:S67-72.
  18. Abdel Razek AA, Kandell AY, Elsorogy LG, Elmongy A, Basett AA. Disorders of cortical formation: MR imaging features. *AJNR Am J Neuroradiol* 2009;30:4-11.
  19. Wang DD, Deans AE, Barkovich AJ, Tihan T, Barbaro NM, Garcia PA, Chang EF. Transmantle sign in focal cortical dysplasia: a unique radiological entity with excellent prognosis for seizure control. *J Neurosurg* 2013;118:337-44.
  20. Salamon N, Kung J, Shaw SJ, Koo J, Koh S, Wu JY, Lerner JT, Sankar R, Shields WD, Engel J Jr, Fried I, Miyata H, Yong WH, Vinters HV, Mathern GW. FDG-PET/MRI coregistration improves detection of cortical dysplasia in patients with epilepsy. *Neurology* 2008;71:1594-601.
  21. Zijlmans M, de Kort GA, Witkamp TD, Huiskamp GM, Seppenwoolde JH, van Huffelen AC, Leijten FS. 3T versus 1.5T phased-array MRI in the presurgical work-up of patients with partial epilepsy of uncertain focus. *J Magn Reson Imaging* 2009;30:256-62.
  22. Knake S, Triantafyllou C, Wald LL, Wiggins G, Kirk GP, Larsson PG, Stufflebeam SM, Foley MT, Shiraishi H, Dale AM, Halgren E, Grant PE. 3T phased array MRI improves the presurgical evaluation in focal epilepsies: a prospective study. *Neurology* 2005;65:1026-31.
  23. Edelstein WA, Glover GH, Hardy CJ, Redington RW. The intrinsic signal-to-noise ratio in NMR imaging. *Magn Reson Med* 1986;3:604-18.
  24. Besson P, Andermann F, Dubeau F, Bernasconi A. Small focal cortical dysplasia lesions are located at the bottom of a deep sulcus. *Brain* 2008;131:3246-55.
  25. Tassi L, Colombo N, Garbelli R, Francione S, Lo Russo G, Mai R, Cardinale F, Cossu M, Ferrario A, Galli C, Bramero M, Citterio A, Spreafico R. Focal cortical dysplasia: neuropathological subtypes, EEG, neuroimaging and surgical outcome. *Brain* 2002;125:1719-32.
  26. Von Oertzen J, Urbach H, Jungbluth S, Kurthen M, Reuber M, Fernández G, Elger CE. Standard magnetic resonance imaging is inadequate for patients with refractory focal epilepsy. *J Neurol Neurosurg Psychiatry* 2002;73:643-7.
  27. Whitwell JL. Voxel-based morphometry: an automated technique for assessing structural changes in the brain. *J Neurosci* 2009;29:9661-4.
  28. Ashburner J, Friston KJ. Voxel-based morphometry--the methods. *Neuroimage* 2000;11:805-21.
  29. Ashburner J. SPM: a history. *Neuroimage* 2012;62:791-800.
  30. Keller SS, Roberts N. Voxel-based morphometry of temporal lobe epilepsy: an introduction and review of the literature. *Epilepsia* 2008;49:741-57.
  31. Friston KJ, Worsley KJ, Frackowiak RS, Mazziotta JC, Evans AC. Assessing the significance of focal activations using their spatial extent. *Hum Brain Mapp* 1994;1:210-20.

32. Genovese CR, Lazar NA, Nichols T. Thresholding of statistical maps in functional neuroimaging using the false discovery rate. *Neuroimage* 2002;15:870-8.
33. Huppertz HJ, Grimm C, Fauser S, Kassubek J, Mader I, Hochmuth A, Spreer J, Schulze-Bonhage A. Enhanced visualization of blurred gray-white matter junctions in focal cortical dysplasia by voxel-based 3D MRI analysis. *Epilepsy Res* 2005;67:35-50.
34. Bernasconi A, Antel SB, Collins DL, Bernasconi N, Olivier A, Dubeau F, Pike GB, Andermann F, Arnold DL. Texture analysis and morphological processing of magnetic resonance imaging assist detection of focal cortical dysplasia in extra-temporal partial epilepsy. *Ann Neurol* 2001;49:770-5.
35. Colliot O, Mansi T, Bernasconi N, Naessens V, Klironomos D, Bernasconi A. Segmentation of focal cortical dysplasia lesions on MRI using level set evolution. *Neuroimage* 2006;32:1621-30.
36. House PM, Lanz M, Holst B, Martens T, Stodieck S, Huppertz HJ. Comparison of morphometric analysis based on T1- and T2-weighted MRI data for visualization of focal cortical dysplasia. *Epilepsy Res* 2013;106:403-9.
37. Braga B, Yasuda CL, Cendes F. White Matter Atrophy in Patients with Mesial Temporal Lobe Epilepsy: Voxel-Based Morphometry Analysis of T1- and T2-Weighted MR Images. *Radiol Res Pract* 2012;2012:481378.
38. Focke NK, Symms MR, Burdett JL, Duncan JS. Voxel-based analysis of whole brain FLAIR at 3T detects focal cortical dysplasia. *Epilepsia* 2008;49:786-93.
39. Rugg-Gunn FJ, Boulby PA, Symms MR, Barker GJ, Duncan JS. Imaging the neocortex in epilepsy with double inversion recovery imaging. *Neuroimage* 2006;31:39-50.
40. Dousset V, Grossman RI, Ramer KN, Schnall MD, Young LH, Gonzalez-Scarano F, Lavi E, Cohen JA. Experimental allergic encephalomyelitis and multiple sclerosis: lesion characterization with magnetization transfer imaging. *Radiology* 1992;182:483-91.
41. Dale AM, Fischl B, Sereno MI. Cortical surface-based analysis. I. Segmentation and surface reconstruction. *Neuroimage* 1999;9:179-94.
42. Fischl B, Sereno MI, Dale AM. Cortical surface-based analysis. II: Inflation, flattening, and a surface-based coordinate system. *Neuroimage* 1999;9:195-207.
43. Fischl B, Dale AM. Measuring the thickness of the human cerebral cortex from magnetic resonance images. *Proc Natl Acad Sci U S A* 2000;97:11050-5.
44. Blackmon K, Kuzniecky R, Barr WB, Snuderl M, Doyle W, Devinsky O, Thesen T. Cortical Gray-White Matter Blurring and Cognitive Morbidity in Focal Cortical Dysplasia. *Cereb Cortex* 2014. [Epub ahead of print].
45. Jackson GD, Connelly A, Duncan JS, Grünewald RA, Gadian DG. Detection of hippocampal pathology in intractable partial epilepsy: increased sensitivity with quantitative magnetic resonance T2 relaxometry. *Neurology* 1993;43:1793-9.
46. Duncan JS, Bartlett P, Barker GJ. Technique for measuring hippocampal T2 relaxation time. *AJNR Am J Neuroradiol* 1996;17:1805-10.
47. Woermann FG, Barker GJ, Birnie KD, Meencke HJ, Duncan JS. Regional changes in hippocampal T2 relaxation and volume: a quantitative magnetic resonance imaging study of hippocampal sclerosis. *J Neurol Neurosurg Psychiatry* 1998;65:656-64.
48. Pell GS, Briellmann RS, Waites AB, Abbott DE, Jackson GD. Voxel-based relaxometry: a new approach for analysis of T2 relaxometry changes in epilepsy. *Neuroimage* 2004;21:707-13.
49. Alexander AL, Lee JE, Lazar M, Field AS. Diffusion tensor imaging of the brain. *Neurotherapeutics* 2007;4:316-29.
50. Mori S, Zhang J. Principles of diffusion tensor imaging and its applications to basic neuroscience research. *Neuron* 2006;51:527-39.
51. Le Bihan D, Mangin JF, Poupon C, Clark CA, Pappata S, Molko N, Chabriat H. Diffusion tensor imaging: concepts and applications. *J Magn Reson Imaging* 2001;13:534-46.
52. Smith SM, Jenkinson M, Johansen-Berg H, Rueckert D, Nichols TE, Mackay CE, Watkins KE, Ciccarelli O, Cader MZ, Matthews PM, Behrens TE. Tract-based spatial statistics: voxelwise analysis of multi-subject diffusion data. *Neuroimage* 2006;31:1487-505.
53. Focke NK, Yogarajah M, Bonelli SB, Bartlett PA, Symms MR, Duncan JS. Voxel-based diffusion tensor imaging in patients with mesial temporal lobe epilepsy and hippocampal sclerosis. *Neuroimage* 2008;40:728-37.
54. Winston GP, Micallef C, Symms MR, Alexander DC, Duncan JS, Zhang H. Advanced diffusion imaging sequences could aid assessing patients with focal cortical dysplasia and epilepsy. *Epilepsy Res* 2014;108:336-9.
55. Riney CJ, Chong WK, Clark CA, Cross JH. Voxel based morphometry of FLAIR MRI in children with intractable focal epilepsy: implications for surgical intervention. *Eur J Radiol* 2012;81:1299-305.
56. Wilke M, Kassubek J, Ziyeh S, Schulze-Bonhage A, Huppertz HJ. Automated detection of gray matter malformations using optimized voxel-based morphometry: a systematic approach. *Neuroimage* 2003;20:330-43.

57. Bonilha L, Montenegro MA, Rorden C, Castellano G, Guerreiro MM, Cendes F, Li LM. Voxel-based morphometry reveals excess gray matter concentration in patients with focal cortical dysplasia. *Epilepsia* 2006;47:908-15.
58. Colliot O, Bernasconi N, Khalili N, Antel SB, Naessens V, Bernasconi A. Individual voxel-based analysis of gray matter in focal cortical dysplasia. *Neuroimage* 2006;29:162-71.
59. Bruggemann JM, Wilke M, Som SS, Bye AM, Bleasel A, Lawson JA. Voxel-based morphometry in the detection of dysplasia and neoplasia in childhood epilepsy: limitations of grey matter analysis. *J Clin Neurosci* 2009;16:780-5.
60. Pail M, Mareček R, Hermanová M, Slaná B, Tyrlíková I, Kuba R, Brázdil M. The role of voxel-based morphometry in the detection of cortical dysplasia within the temporal pole in patients with intractable mesial temporal lobe epilepsy. *Epilepsia* 2012;53:1004-12.
61. Kassubek J, Huppertz HJ, Spreer J, Schulze-Bonhage A. Detection and localization of focal cortical dysplasia by voxel-based 3-D MRI analysis. *Epilepsia* 2002;43:596-602.
62. Wagner J, Weber B, Urbach H, Elger CE, Huppertz HJ. Morphometric MRI analysis improves detection of focal cortical dysplasia type II. *Brain* 2011;134:2844-54.
63. Huppertz HJ, Wagner J, Weber B, House P, Urbach H. Automated quantitative FLAIR analysis in hippocampal sclerosis. *Epilepsy Res* 2011;97:146-56.
64. Abbott DF, Pell GS, Pardoe H, Jackson GD. Voxel-based iterative sensitivity (VBIS) analysis: methods and a validation of intensity scaling for T2-weighted imaging of hippocampal sclerosis. *Neuroimage* 2009;44:812-9.
65. Bernasconi A, Bernasconi N, Caramanos Z, Reutens DC, Andermann F, Dubeau F, Tampieri D, Pike BG, Arnold DL. T2 relaxometry can lateralize mesial temporal lobe epilepsy in patients with normal MRI. *Neuroimage* 2000;12:739-46.
66. Bartlett PA, Symms MR, Free SL, Duncan JS. T2 relaxometry of the hippocampus at 3T. *AJNR Am J Neuroradiol* 2007;28:1095-8.
67. Eriksson SH, Rugg-Gunn FJ, Symms MR, Barker GJ, Duncan JS. Diffusion tensor imaging in patients with epilepsy and malformations of cortical development. *Brain* 2001;124:617-26.
68. Thesen T, Quinn BT, Carlson C, Devinsky O, DuBois J, McDonald CR, French J, Leventer R, Felsovalyi O, Wang X, Halgren E, Kuzniecky R. Detection of epileptogenic cortical malformations with surface-based MRI morphometry. *PLoS One* 2011;6:e16430.
69. Rugg-Gunn FJ, Eriksson SH, Boulby PA, Symms MR, Barker GJ, Duncan JS. Magnetization transfer imaging in focal epilepsy. *Neurology* 2003;60:1638-45.
70. Kadom N, Trofimova A, Vezina GL. Utility of magnetization transfer T1 imaging in children with seizures. *AJNR Am J Neuroradiol* 2013;34:895-8.
71. Focke NK, Bonelli SB, Yogarajah M, Scott C, Symms MR, Duncan JS. Automated normalized FLAIR imaging in MRI-negative patients with refractory focal epilepsy. *Epilepsia* 2009;50:1484-90.
72. Rugg-Gunn FJ, Boulby PA, Symms MR, Barker GJ, Duncan JS. Whole-brain T2 mapping demonstrates occult abnormalities in focal epilepsy. *Neurology* 2005;64:318-25.
73. Kosior RK, Sharkey R, Frayne R, Federico P. Voxel-based relaxometry for cases of an unresolved epilepsy diagnosis. *Epilepsy Res* 2012;99:46-54.
74. Rugg-Gunn FJ, Eriksson SH, Symms MR, Barker GJ, Duncan JS. Diffusion tensor imaging of cryptogenic and acquired partial epilepsies. *Brain* 2001;124:627-36.
75. Rugg-Gunn FJ, Eriksson SH, Symms MR, Barker GJ, Thom M, Harkness W, Duncan JS. Diffusion tensor imaging in refractory epilepsy. *Lancet* 2002;359:1748-51.
76. Colliot O, Antel SB, Naessens VB, Bernasconi N, Bernasconi A. In vivo profiling of focal cortical dysplasia on high-resolution MRI with computational models. *Epilepsia* 2006;47:134-42.
77. Salmenpera TM, Symms MR, Rugg-Gunn FJ, Boulby PA, Free SL, Barker GJ, Yousry TA, Duncan JS. Evaluation of quantitative magnetic resonance imaging contrasts in MRI-negative refractory focal epilepsy. *Epilepsia* 2007;48:229-37.
78. Wang ZI, Alexopoulos AV, Jones SE, Najm IM, Ristic A, Wong C, Prayson R, Schneider F, Kakisaka Y, Wang S, Bingaman W, Gonzalez-Martinez JA, Burgess RC. Linking MRI postprocessing with magnetic source imaging in MRI-negative epilepsy. *Ann Neurol* 2014;75:759-70.
79. Barron DS, Fox PM, Laird AR, Robinson JL, Fox PT. Thalamic medial dorsal nucleus atrophy in medial temporal lobe epilepsy: A VBM meta-analysis. *Neuroimage Clin* 2012;2:25-32.

**Cite this article as:** Martin P, Bender B, Focke NK. Post-processing of structural MRI for individualized diagnostics. *Quant Imaging Med Surg* 2015;5(2):188-203. doi: 10.3978/j.issn.2223-4292.2015.01.10